J.of Metastable and Nanocrystalline Materials Vol.15-16(2003), 607-614.

CHARACTERIZATION OF BULK CEMENTITE PRODUCED BY MECHANICAL ALLOYING AND SPARK PLASMA SINTERING

M. Umemoto, Y. Todaka, T. Takahashi, P. Li, R. Tokumiya and K. Tsuchiya

Department of Production Systems Engineering, Toyohashi University of Technology, Tempaku-cho, Toyohashi 441-8580, Japan

Keywords: Cementite, Mechanical Properties, Characterization, Mechanical Alloying MA, Sintering

Abstract Using the bulk cementite (Fe_3C, θ) fabricated by mechanical alloying (MA) and spark plasma sintering (SPS), the mechanical properties of cementite such as Young's modulus, hardness and compression strength were measured. The abnormal decrease in Young's modulus and the abnormal increase in hardness with a decrease of temperature were observed at around the Curie temperature. It has been found that the hardness and Young's modulus of the alloyed cementite increased in the order of V, Cr, Mn and Mo. At elevated temperatures, cementite could deform in compression superplastically to large strain without cracks. Multilayers of cementite and ferrite with the layer thickness less than 100 μm could be fabricated by compression at elevated temperatures and this indicated a cooperative deformation of these two phases.

Introduction

Cementite is one of the most well known metastable phases in steels [1]. Most of the commercial carbon steels consist of ferrite and a few mass% of cementite. Thus several millions tons of cementite have been commercially produced every year as a second phase of steels. Once cementite solidifies with eutectic reaction or precipitates from austenite or from ferrite, it is quite stable as long as it is embedded in austenite or ferrite matrix since its decomposition to ferrite + graphite accompanies a large volume expansion (about 14 %). Thus, in most of the cases the metastable nature of cementite is not realized. Furthermore, although the precise strength of cementite has not been known; not many practical problems have arisen since cementite is more than 10 times stronger [2] than conventional ferrite. However, recent development of high strength steels requires the precise characteristics of cementite. In the high strength pearlitic wire, the work-hardening behavior of pearlite cannot be understood without knowing the deformation behavior of cementite [3]. In the ultra fine grained steels, the strength of ferrite increased to comparable level with that of cementite [4]. However, the properties of cementite could not been studied in detail since it has not been possible to obtain large samples of cementite. In our previous paper [5-7], we have reported the successful fabrication of bulk cementite of centimeter-size by combining mechanical alloying (MA) with spark plasma sintering (SPS). Various physical properties have been obtained for pure and alloyed bulk cementite specimens [5-7].

The purpose of the present study is to report the mechanical properties of cementite measured using bulk samples. The hardness, Young's modulus, compression strength and their temperature dependence were measured and compared with those of pure Fe.

Experimental Procedures

Pure Fe, graphite as well as Cr, Mn, Mo, V were mixed at compositions of $(Fe_{1-x}M_x)_{75}C_{25}$ (M=Cr, Mn; x = 0.1, 0.2 and 0.3, for M=V, Mo; x = 0.1). The MA powders were subjected to spark plasma sintering (SPS) at 1173 K for 900 s at a stress of 50 MPa in vacuum. Structural characterizations (XRD and SEM) were performed on the sintered compacts. SEM observations were performed on the sintered compacts polished and etched by 0.5 g $CuCl_2$ + 10 ml HCl. The microhardness of the sintered compacts was measured under a load of 0.98 N for 15 s. Compression test of the sintered compacts was carried out at a strain rate of 2.14×10^{-3} s^{-1}. The Young's modulus, *E*, was measured by a piezoelectric composite-bar method of a plate specimen.

Results and Discussion

Sintered compact and microstructure

Figure 1 shows a sintered compact prepared in the present study. The size of the sample (ϕ50 x 6 mm) is large enough for most of the measurements. Figure 2 shows the SEM micrograph of a sintered compact $(Fe_{0.8}Mn_{0.2})_3C$ after polished and etched. The grain boundaries of the cementite can be observed clearly after etched by the solution of 0.5 g $CuCl_2$ + 10 ml HCl. Grain size of the bulk cementite produced is around 0.5 μm. The porosities (seen as black) are less than 5 vol%. A micro-Vicker's indentation mark made by a load of 0.98 N is also shown in Fig.2. The indentation mark covers about 100 g which is large enough to average the orientation dependence of hardness. Figure 3 shows the TEM micrographs of $(Fe_{0.95}Mn_{0.05})_3C$ specimen. Grain boundaries of cementite look similar to those of ferrite. Planer defects, probably stacking faults, are observed as indicated by the arrow. Besides the planer defects, small voids are seen at grain boundaries and inside grains.

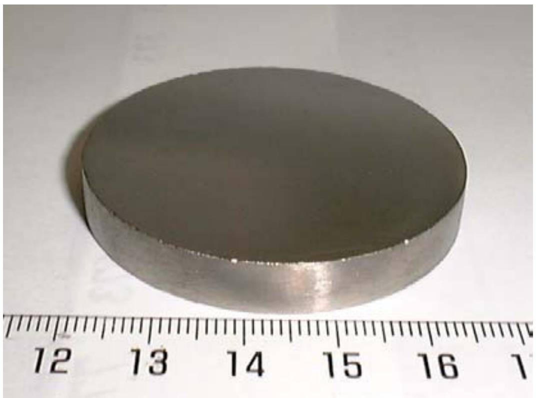

Fig. 1 Bulk cementite ($(Fe_{0.95}Mn_{0.05})_3C$) produced by sintering MA powder.

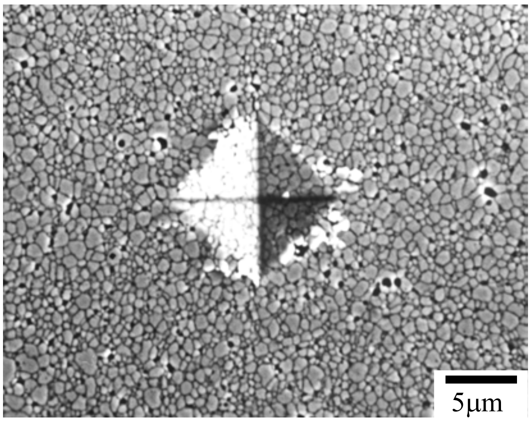

Fig. 2 SEM micrograph of a typical indentation mark on bulk cementite sample of $(Fe_{0.8}Mn_{0.2})_3C$ with load 0.98 N and hardness 13.3 GPa.

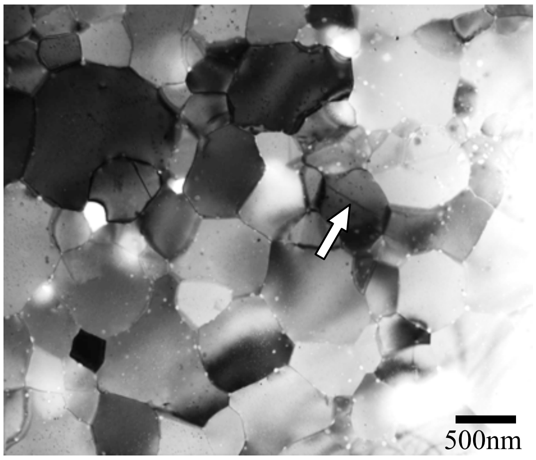

Fig. 3 TEM micrograph of bulk cementite ($(Fe_{0.95}Mn_{0.05})_3C$). Stacking faults (arrow) are sometimes observed.

Elastic modulus of cementite

Young's modulus, *E*, of bulk cementite at room temperature was measured to be 191 GPa which is smaller than that of pure Fe measured with the same method (212 GP a). Drapkin and Fokin [8] have measured Young's modulus of iron-cementite alloys with different carbon content up to 2.7 wt%, and estimated Young's modulus of cementite to be about 180 GPa and pointed out that this is

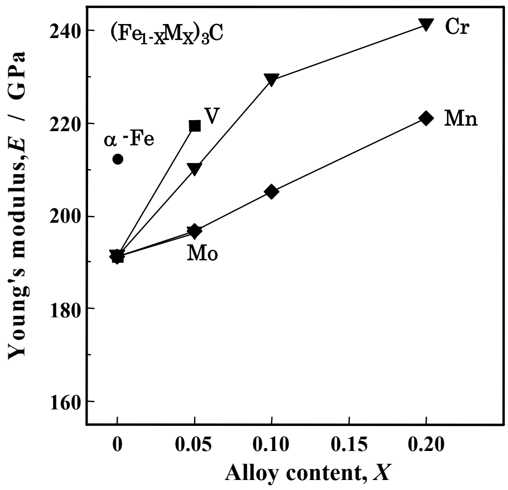

Fig. 4 Effect of alloying additions on Young's modulus of cementite.

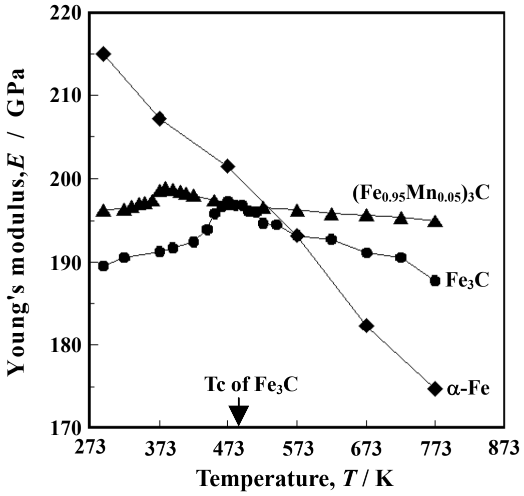

Fig. 5 Temperature variation of Young's modulus of Fe_3C, $(Fe_{0.95}Mn_{0.05})_3C$ and α-Fe.

lower than that of pure Fe (216 GPa). This behavior is quite different from most of other carbides, which show a much higher Young's modulus than their pure metal counterparts.

A roughly linear increase of *E* with the increase of alloying content was observed as is shown in Fig. 4. The effect of Mo and Mn additions on the increase in *E* is almost the same, while a much larger increase was obtained for Cr and V additions. V addition of 5 % increased the *E* of the cementite from 191 GPa to 220 GPa, which is the same level as that of pure Fe.

The temperature dependence of *E* of the bulk cementite was measured from room temperature to 773 K for Fe_3C and $(Fe_{0.95}Mn_{0.05})_3C$ and is shown in Fig. 5 together with that of pure Fe measured with the same equipment. It is seen that the temperature dependence of *E* of the cementite above its Curie temperature (483 K) is smaller than that of pure Fe (about 1/3). Below the Curie temperature *E* decrease with temperature. This is known as ΔE effect, which is the decrease of *E* in accordance with the magnetic transition from the paramagnetic to ferromagnetic state [9]. The small temperature dependence of *E* of the cementite is quite abnormal. The ratio of β(= dE/dT) to linear thermal expansion coefficient α, β/α is a constant value for a given crystal structure (-25.5 for bcc and -17.9 for fcc crystals [9]). However, the β/α of cementite is -6.87 (above T_C). This is mainly due to the low β value.

Scott *et al.* [10] have measured the bulk modulus of cementite by measuring the lattice parameters using synchrotron X-ray diffraction under pressure generated in a diamond anvil cell. They found that the bulk modulus of cementite is 175 GPa. Using this value, various elastic moduli can be estimated as listed in Table 1. Here cementite was assumed to be isotropic, although it is known to be anisotropic.

Table 1 Elastic moluli of pure cementite comparing with α-Fe.

	Cementite	α -Fe
Young's modules E [GPa]	**190**	**211**
Shear modules G [GPa]	**(72.0)**	**81.6**
Bulk modules K [GPa]	**175±4**	**172**
Poisson's ratio ν	**(0.32)**	**0.295**

Vicker's microhardness

Vicker's microhardness of the sintered compacts at room temperature was measured and is shown in Fig. 6 as a function of alloying content. The hardness of alloyed cementite increased in the order of V, Cr, Mn and Mo. This evolution is in good agreement with the previous study on pro-eutectoid cementite [11], though those values for pro-eutectoid were 2-3 GPa higher than the present results. A part of this difference arises from the voids in the sintered compacts used in the

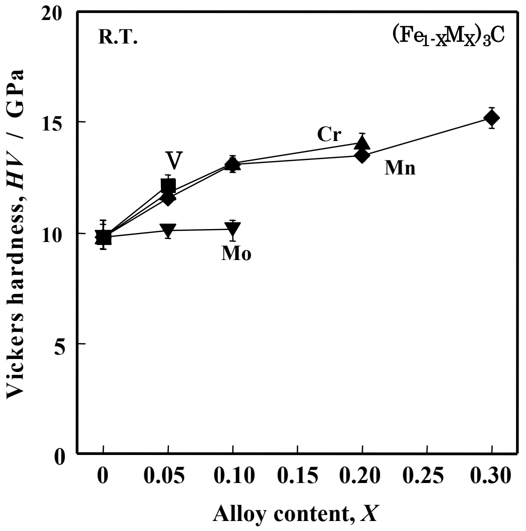

Fig. 6 Effect of alloying addition on the room temperature hardness of cementite.

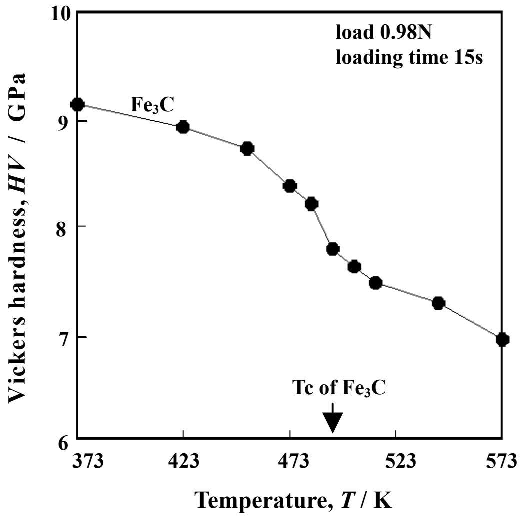

Fig. 7 Temperature dependence of hardness of bulk Fe_3C.

present study. However, the previous data obtained from cementite in cast iron or steels may contain errors arising from small load and effect of soft matrix.

Figure 7 shows the temperature variation of hardness in pure Fe_3C. The abnormal hardness decrease with temperature was observed at around the Curie temperature. As mentioned above, Young's modulus of the cementite increases with temperature in this temperature range. Thus this abnormal decrease in hardness is not associated with the change in elastic properties and must be related to the plastic properties of cementite. Similar abnormal hardness change in cementite was reported by Yakushiji *et al.*[12] They measured the hardness of primary cementite in the directionally solidified hypereutectic Fe-4.5%C alloy. They observed discontinuous decrease in hardness from 473 to 523 K. It should be noted this abnormal change in hardness is observed below and above the Curie temperature and not only below the Curie temperature like the case of Young's modulus or thermal expansion. Figure 8 shows the microhardness change of the 5 % alloyed cementite as a function of temperature. Clear alloying effect is seen in the temperature dependence on hardness. Alloyed cementite has a higher hardness than the unalloyed one at all the temperatures studied. However, the alloying element effect on the hardness is different at room temperature and at 773 K. At 773 K, the hardness is high in the order of Mo, V, Cr and Mn. The creep deformation was realized at 773 K from the clear hardness dependence on loading time. It is known that in creep deformation solid solution strengthening of ferrite or austenite increases with the increasing misfit parameter of atomic radii. The misfit parameters for Mo, V, Cr and Mn with Fe are 0.084, 0.034, 0.014 and 0.016, respectively. It is interesting to note that the hardness of alloyed cementite at 773 K is well correlated with the misfit parameter of atomic radii as observed in ferrite and austenite. The abnormal hardness decrease was also observed in all the alloyed cementite around their Curie temperatures as is shown in Fig. 8. The abnormal change in hardness is less pronounced in alloyed cementite

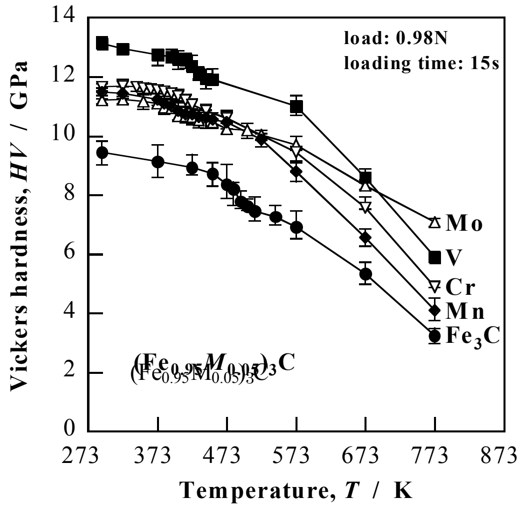

Fig. 8 The temperature dependence of microhardness of the sintered Cr, Mn, Mo and V alloyed cementite compacts.

studied. This might corresponds to the decrease in magnetization by alloying these elements. The cause of this hardness variation near the Curie temperature remains uncertain.

Compression test

The true stress-true strain curves obtained from the compression tests of cementite tested at room temperature and 773 K are shown in Fig. 9. At room temperature, cementite fractured within the elastic limit. The maximum true stress increased with alloy addition especially with Cr. At 773 K, plastic strain of about 0.1 was observed in most of the specimens. Cr alloyed specimen showed very high flow stress of about 3 GPa at 773 K.

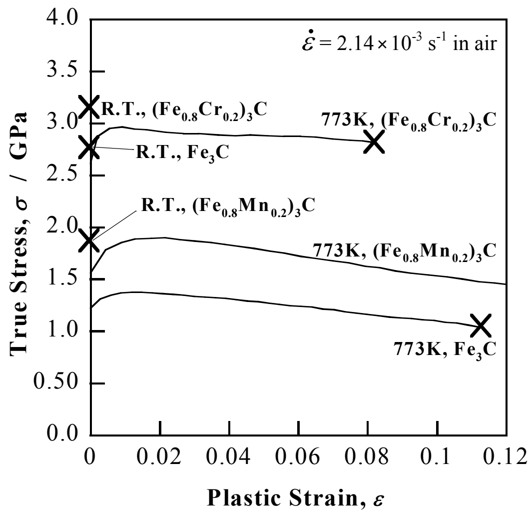

Fig. 9 Compressive stress-strain curves of pure and alloyed cementite at room temperature and 773 K.

High temperature deformation

Kim *et al.* [13] have reported that a fine grained cementite-based material exhibits superplastic properties. They prepared a fine grained (linear intercept grain size of 2.1 μm) material contains 80 vol% cementite from gas atomized Fe-5.25%C-1.5%Cr powder. The tensile elongation as large as 600 % was obtained. At 998 K(below the A_1) the strain rate of 3x10^{-4} s^{-1} was observed under the stress of 100 MPa. It is expected that the present bulk cementite may exhibit superplastic behavior since the grain size is much smaller than theirs. A preliminary compression test was carried out at a constant pressure of 100 MPa to $(Fe_{0.95}Mn_{0.05})_3C$ sample with initial linear intercept grain size of 0.41 μm. Figure 10 shows a specimen before and after the compression test. The initial height of the specimen was 5.3 mm and a final height was 0.76 mm. The obtained compression strain is -1.94 and this is equivalent to a tensile elongation of 600 %. In spite of such a large deformation, no cracks were observed either on the surface or in the interior of the sample. The hardness of the sample did not change (12.1 and 12.6 GPa at room temperature before and after deformation, respectively). It is interesting to note that the present bulk cementite can deformed with a sufficiently high strain rate (about 0.06 s^{-1}) at the stress of 0.1 GPa at 973 K although it has a strength about 4 GPa at room temperature. Figure 11 shows a cross-sectional SEM micrographs

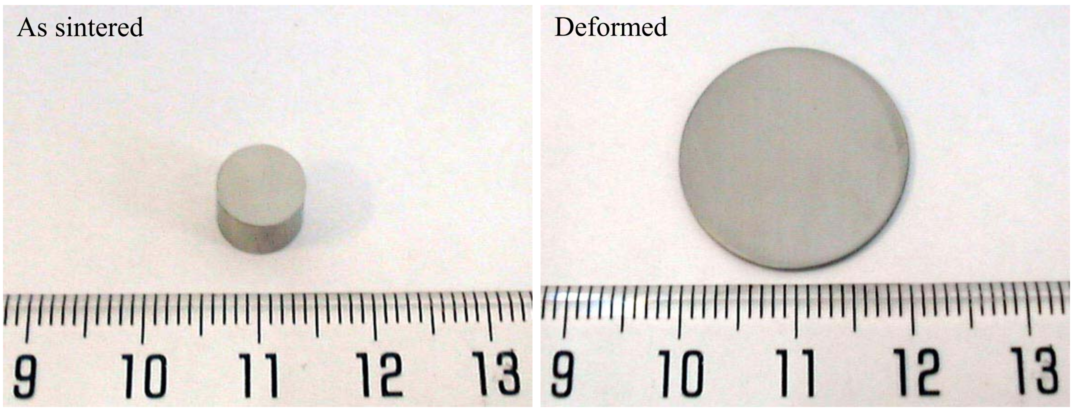

(a) (b)

Fig. 10 Specimen before (a) and after (b) the compression (at 973 K, 100 MPa kept for 3.6 ks).

from the center of the sample before and after the compression test. The grains are slightly elongated along the direction perpendicular to the compression axis (vertical in the figure) and cavities were observed around grain boundaries. The TEM observation from the compression direction showed clear grain growth from 0.46 to 1.5 μm as is shown in Fig. 12. Dislocations are scarcely observed in the grains. No traces of decompositions of cementite were recognized. The present sample does not contain any second phase (except a few vol% of voids) which could prevent the grain growth, the cementite grains grew with a sufficiently high rate. These observations suggest that the present fine grained bulk cementite specimen deformed mostly by grain-boundary sliding mechanism and partly by a slip deformation mechanism. This results, strongly suggests that during sintering the MA powder, superplastic deformation takes place and it assisted the consolidation.

Although the forming of bulk cementite can be done at elevated temperatures, bulk cementite is essentially brittle at room temperature. This limits the application of bulk cementite. It is desired to produce cementite composites with ductile materials. In the present study, cementite / low carbon steel multilayers were produced. Cementite discs of 6 mm in diameter and 0.45 mm thick cut from the sintered bulk cementite and low carbon (Fe-0.25%C or Fe-0.15%C) discs of 6 mm in diameter and 0.90 mm in thickness were stacked alternatively. After stacking, the sample is compressed at 873 K at the initial stress of 100 MPa. The result is shown in Fig. 13, where 3 layers of $(Fe_{0.95}Mn_{0.05})_3C$ and 4 layers of fine grained (about 1 μm) Fe-0.15%C steel discs were stacked initially and compressed to 66 % in reduction. It is seen that low carbon steel and cementite

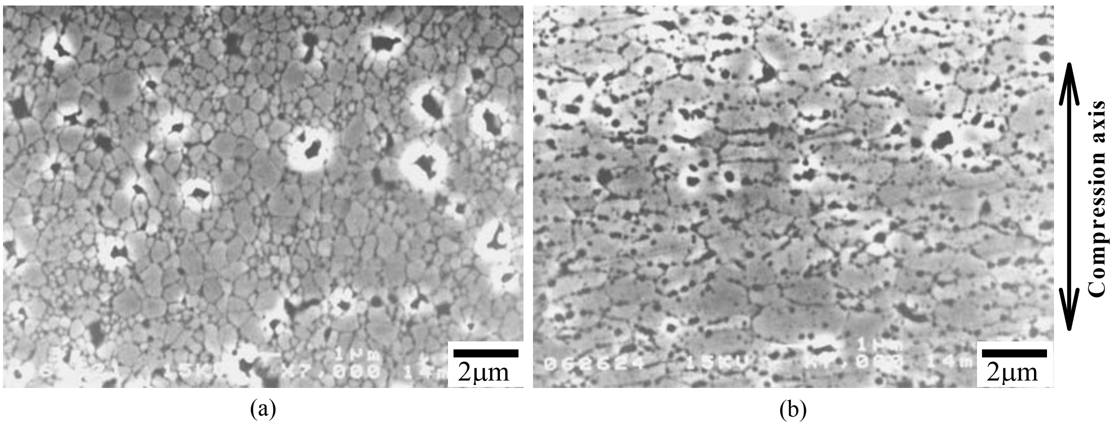

Fig. 11 SEM micrographs of the specimen before (a) and after (b) the compression (at 973 K, 100 MPa kept for 3.6 ks).

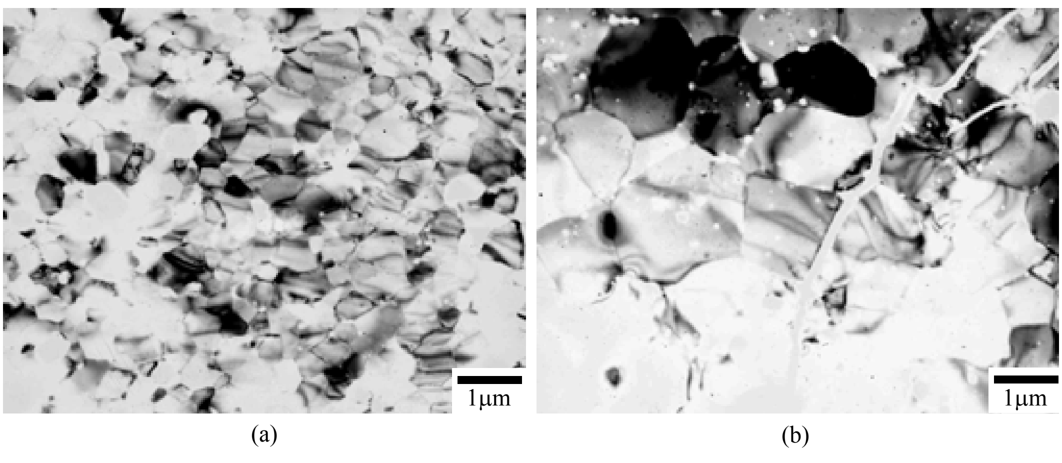

Fig. 12 TEM micrographs of the specimen before (a) and after (b) the compression. The compression was carried out at 973 K with the stress of 100 MPa.

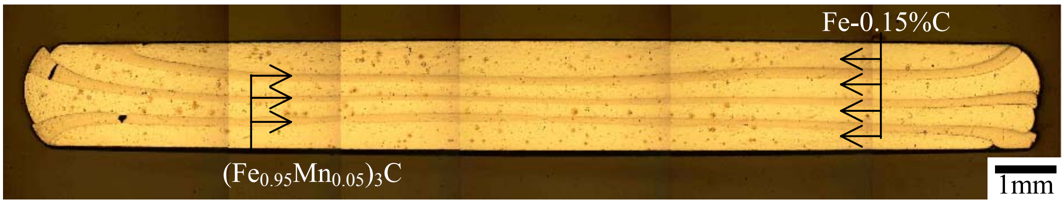

Fig. 13 Cementite / low carbon (Fe-0.15%C) steel multilayers produced by compression at 873 K with the stress of 100 MPa.

deformed uniformly. Cracks or necking of cementite layers are hardly observed. Such cooperative deformation of low carbon steel with bulk cementite was observed even in a coarse grained (about 20 μm) low carbon samples. Figure 14 shows a cross-sectional SEM micrograph of cementite and low carbon (commercial Fe-0.25%C) compressed at 873 K at the stress of 100 MPa. The grain size of low carbon steel is about 5 μm which was initially about 20 μm. The thickness of cementite is about 40 μm which was initially 700 μm. There are no voids or cavities at the cementite / low carbon steel interfaces. The irregularity of the interface corresponds to the grain size of cementite instead of low carbon steel. It seems that the grain size of low carbon steel becomes fine by recrystallization and grain boundary sliding will become a dominant deformation mechanism in low carbon steel layers.

As an application of cementite and low carbon steel laminates, a knife was made as is shown in Fig. 15. Cementite layer was sandwiched between the two layers of low carbon steel. The cutting edge is a hard cementite and two side layers are ductile low carbon steel which protect cementite from fracture. The hardness of cutting edge is 12 GPa and hard enough to be used as a glass cutter.

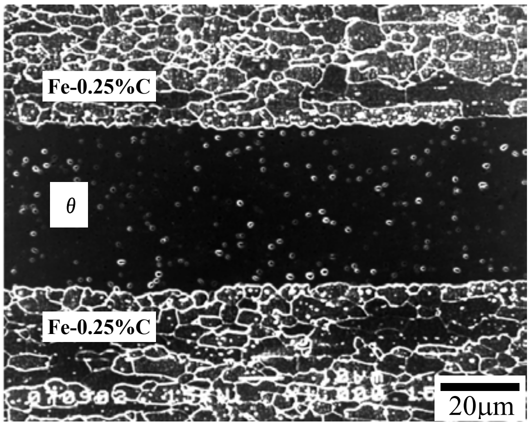

Fig. 14 SEM image of cementite / low carbon steel (commercial Fe-0.25%C) multilayers produced by compression at 873 K with the stress of 100 MPa.

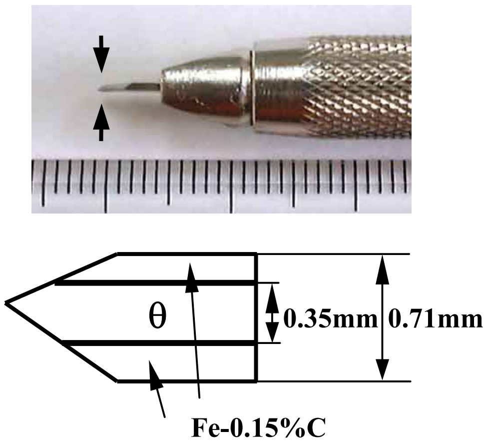

Fig. 15 A glass cutter made of cementite / low carbon laminates.

Summary

In the present study, using bulk cementite samples produced by mechanical allying of the elemental powders and spark plasma sintering of MA powders, the temperature dependence of Young's modulus, hardness, compression strength of cementite were measured. Young's modulus of cementite exhibited abnormal negative temperature dependence below its Curie temperature due to ΔE effect. Young's modulus of paramagnetic cementite showed very small temperature dependence. The hardness of the cementite showed an abnormal decrease with temperature at around its Curie temperature. Compression test showed high strength of the cementite especially when alloyed with Cr. It also showed the brittle nature of cementite as observed in cast irons. At elevated temperatures, bulk cementite exhibited superplastic deformation when compressed at stress in the range of 100-150 MPa. This superplastic deformation is due to its small grain size around 0.5 μm. As a cementite composite with ductile material, cementite / low carbon steel multilayers were fabricated using the superplastic deformation. A glass cutter made of cementite / low carbon steel laminates was demonstrated as an application of the technique developed in the present study.

Acknowledgement

This work is partly supported by the Grant-in-Aid by the Japan Society for the Promotion of Science. The authors express their gratitude to Prof. Y. Tomota at Ibaraki University for compression test.

References

[1] L.S.Darken and R.W.Gurry: *AIME Trans.* (1951), p.1015.
[2] M.J.Collins and D.A.Woodford: Journal of the iron and steel institute (1965), p.184.
[3] G.Langford: Met. Trans. Vol.8A (1977), p.861.
[4] H.Hidaka, T.Suzuki, Y.Kimura and S.Takaki: Mater. Sci. Forum Vols.304-306 (1999), p.115.
[5] M.Umemoto, Z.G.Liu, H.Takaoka, M.Sawakami, K.Tsuchiya and K.Masuyama: Metall. Mater. Trans. A Vol.32 (2001), p.2127.
[6] M.Umemoto, Z.G.Liu, K.Masuyama and K.Tsuchiya: Scripta Mater. Vol.45 (2001), p.391.
[7] M.Umemoto, Z.G.Liu, D.Y.Liu, H.Takaoka and K.Tsuchiya: Mater. Sci. Forum Vols.386-388, (2002), p.199.
[8] B.M.Drapkin and B.V.Fokin: Phys. Met. Metall, Vol.49 (1980), p.177.
[9] A.Kagawa, T.Okamoto and H.Matsumoto: Acta Metall. Vol.35 (1987), p.797.
[10] H.P.Scott, Q.Williams, E.Knittle: Geophys. Res. Lett. Vol.28 (2001), p.1875.
[11] A.Inoue, T.Ogura and T.Masumoto: Bull. Japan Inst. Metals Vol.13 (1974), p.653.
[12] M.Yakushiji, Y.Kondo, H.Matsumoto and T.Okamoto: J. Jpn. Inst. Met., Vol.39 (1975), p.606.
[13] W.J.Kim, J.Wolfenstine, O.A.Ruano, G.Frommeyer and O.D.Sherby: Metall. Trans. A, Vol.23A (1992), p.527.